Robert, B., & Lutz, M. (1986) *Biochemistry 25*, 2303-2309.
Salehi, A., Oertling, W. A., Fonda, H. N., Babcock, G. T., & Chang, C. K. (1988) *Photochem. Photobiol. 48*, 525-530.
Sawatzki, J., Fischer, R., Scheer, H., & Siebert, F. (1990) *Proc. Natl. Acad. Sci. U.S.A. 87*, 5903-5906.
Scheidt, W. R., & Lee, Y. J. (1987) *Struct. Bonding 64*, 1-70.
Schrader, B., & Simon, A. (1988) *Mikrochim. Acta 2*, 227-230.
Schrader, B., Hoffmann, A., Simon, A., Podschadlowski, R., & Tischer, M. (1990) *J. Mol. Struct. 217*, 207-220.
Spiro, T. G., Czernuszewicz, R. S., & Li, X.-Y. (1990) *Coord. Chem. Rev. 100*, 541-571.
Tiede, D. M., Budil, D. E., Tang, J., El-Kabbani, O., Norris, J. R., Chang, C. H., & Schiffer, M. (1988) in *The Photosynthetic Bacterial Reaction Center, Structure and Dynamics* (Breton, J., & Vermeglio, A., Eds.) pp 13-20, Plenum, New York.
Woodbury, N. W., Becker, M., Middendorf, D., & Parson, W. W. (1985) *Biochemistry 24*, 7516-7521.
Yager, P., & Gaber, B. P. (1987) in *Biological Applications of Raman Spectroscopy* (Spiro, T. G., Ed.) Vol. 1, pp 203-261, Wiley-Interscience, New York.
Zhou, Q., Robert, B., & Lutz, M. (1987) *Biochim. Biophys. Acta 890*, 368-376.
Zhou, Q., Robert, B., & Lutz, M. (1989) *Biochim. Biophys. Acta 977*, 10-18.

Cholate-Solubilized Erythrocyte Glucose Transporters Exist as a Mixture of Homodimers and Homotetramers†

Daniel N. Hebert* and Anthony Carruthers*

Program in Molecular Medicine and Department of Biochemistry and Molecular Biology, University of Massachusetts Medical Center, 373 Plantation Street, Worcester, Massachusetts 01605

Received February 20, 1991; Revised Manuscript Received March 15, 1991

ABSTRACT: The molecular size of purified, human erythrocyte glucose transport protein (GLUT1) solubilized in cholic acid was determined by size-exclusion chromatography (SEC) and sucrose gradient ultracentrifugation. GLUT1 purified in the presence of dithiothreitol (GLUT1 + DTT) is resolved as a complex of average Stokes' radius 5.74 nm by SEC. This complex displays D-glucose-inhibitable cytochalasin B binding and, upon reconstitution into proteoliposomes, catalyzes cytochalasin B inhibitable D-glucose transport. GLUT1 purified in the absence of dithiothreitol (GLUT1 - DTT) is resolved by SEC as at least two particles of average Stokes' radii 5.74 (minor component) and 7.48 nm (major component). Solubilization of GLUT1 - DTT in the presence of dithiothreitol reduces the amount of 7.48-nm complex and increases the amount of 5.74-nm complex resolved by SEC. GLUT1 - DTT displays D-glucose-inhibitable cytochalasin B binding and, upon reconstitution into proteoliposomes, catalyzes cytochalasin B inhibitable D-glucose transport. Sucrose gradient ultracentrifugation of GLUT1 + DTT in cholate resolves GLUT1 into two components of 4.8 and 7.6 S. The 4.8S complex is the major component of GLUT1 + DTT. The reverse profile is observed upon sucrose gradient ultracentrifugation of GLUT1 - DTT. SEC of human erythrocyte membrane proteins resolves GLUT1 as a major broad peak of average Stokes' radius 7.48 nm and a minor component of 5.74 nm. Both components are characterized by D-glucose-inhibitable cytochalasin B binding. Purified GLUT1 is associated with approximately 26 tightly bound lipid molecules per monomer of transport protein. These data suggest that purified GLUT1 exists as a mixture of homodimers and homotetramers in cholate–lipid micelles and that the presence of reductant during solubilization favors dimer formation.

The facilitated diffusion of pentose and hexose monosaccharides across cell membranes is mediated by a family of integral membrane glycoproteins called glucose transporters. At least five isoforms of glucose transporter have been identified by using biochemical and recombinant DNA technologies (Mueckler et al., 1985; Birnbaum et al., 1986; Thorens et al., 1988; Kayano et al., 1988; Celenza et al., 1988; James et al., 1989). While advances in this area have been notable, a number of fundamental properties of glucose transport systems remain to be resolved. These include information regarding the secondary and higher order structures of the glucose transport proteins.

In this study we ask whether human erythrocyte glucose transporter (GLUT1)[1] exists as monomeric or as multimeric species in detergent extracts of membranes. Previous, target-size analyses suggest that the cytochalasin B binding and the sugar transport competent components of the human erythrocyte sugar transport system exist as 124- or 220-kDa

† This work was supported by National Institutes of Health Grant DK 36081.

* Author to whom correspondence should be addressed.

[1] Abbreviations: cmc, critical micellular concentration; DTT, dithiothreitol; EDTA, ethylenediaminetetraacetic acid; EPC, egg phosphatidylcholine; GLUT1, human erythrocyte glucose transporter; MOPS, 3-(*N*-morpholino)propanesulfonic acid; PAGE, polyacrylamide gel electrophoresis; SDS, sodium dodecyl sulfate; SEC, size-exclusion chromatography; Tris-HCl, tris(hydroxymethyl)aminomethane hydrochloride.

0006-2960/91/0430-4654$02.50/0

structures (Cuppoletti et al., 1981; Jung et al., 1980; Jarvis et al., 1986).

The results of this current study support the view that the cholate-solubilized human erythrocyte glucose transport system exists as 104- and 226-kDa species and that the presence of reductant during solubilization favors formation of the 104-kDa species.

Materials and Methods

Materials. [^{3}H]Cytochalasin B and [^{14}C]-D-glucose were purchased from New England Nuclear. Rabbit antisera raised against a synthetic carboxyl-terminal peptide of GLUT1 (intracellular residues 480–492; C-IgGs) were obtained from East Acres Biologicals. Anti-GLUT1 antisera reacting exclusively with an extracellular moiety of GLUT1 (δ-IgGs) were prepared as described previously (Harrison et al., 1990). All remaining materials were purchased from Sigma Chemical Co. unless stated otherwise.

Solutions. Saline consisted of 150 mM NaCl, 5 mM Tris-HCl, and 0.2 mM EDTA, pH 7.4. Lysis medium contained 10 mM Tris-HCl and 2 mM EDTA, pH 7.4. Tris medium consisted of 50 mM Tris-HCl and 0.2 mM EDTA, pH 7.4.

Red Cells and Red Cell Ghosts. Red cell ghosts were prepared from washed red cells as in Helgerson et al. (1989). Red cell ghosts were depleted of peripheral membrane proteins by a single alkali wash as in Carruthers (1986a).

Sugar Transport Assays in Proteoliposomes. [U-^{14}C]-α-D-Glucose uptake at 0.1 mM D-glucose ± 10 μM cytochalasin B by reconstituted proteoliposomes at 20 °C was assayed as described previously (Helgerson et al., 1989).

Glucose Transport Protein. GLUT1 plus endogenous lipid were purified from human erythrocytes as described by Cairns et al. (1984). GLUT1 was also purified by omitting DTT (10 mM) from the alkali extraction step, the solubilization step, and during application of solubilized proteins to the DEAE-cellulose column.

ELISA. ELISA was performed by using C- and/or δ-IgGs as described by Carruthers and Helgerson (1989).

Reconstituted Proteoliposomes. Detergent extracts of red cell ghost membranes and of purified GLUT1 were reconstituted into egg phosphatidylcholine (EPC) bilayers by cholate dialysis. EPC (30 mg in hexane) was dried to a thin film under N_2. The lipid film was placed in vacuo for 3 h to remove traces of remaining solvent. The lipid was dissolved in 2 mL of saline plus 32 mg of cholic acid (the minimum amount found necessary to solubilize this amount of EPC) and centrifuged at 34000*g* for 30 min, and the supernatant was placed on ice. GLUT1 (10–100 μg) or red cell membranes (500–5000 μg of protein) were dissolved in saline containing 50 mM cholic acid (±5 mM DTT; cholate:lipid molar ratio ≈ 2) by end over end rotation at 5 °C for 30 min. The sample was centrifuged at 34000*g* for 30 min and the supernatant combined with the solubilized EPC and mixed by end over end rotation at 5 °C for 30 min. The lipid–protein mixture was dialyzed against two changes of 6 L of saline at 5 °C for 24 h. The dialyzed solution was frozen rapidly in dry ice–acetone and then allowed to thaw at room temperature. The resulting proteoliposomes are large (1–3-μm diameter judged by phase contrast microscopy) and are sedimented by centrifugation at 14000*g* for 5 min. Reconstituted GLUT1 was quantitated by using ELISA. The vesicles contain a scrambled orientation (40% right side out, 60 wrong side out) of GLUT1 based upon binding of δ- and C-terminal antisera to intact and Triton X-100 solubilized proteoliposomes.

Photolabeling GLUT1 Using [^{3}H]Cytochalasin B. Red cells, red cell ghosts, and purified GLUT1 were preincubated in saline or Tris medium containing [^{3}H]cytochalasin B (3.7 μM, 50 μCi) plus 10 μM cytochalasin D ± D- or L-glucose (200 mM) for 20 min on ice. The suspension was irradiated at 300 nm for 0.5–5 min in a Rayonett photoreactor and centrifuged at 34000*g* for 20 min, the supernatant was aspirated, and the cells or membranes were resuspended in 10–100 volumes of saline or Tris medium. The centrifugation/wash cycle was repeated twice more.

Nondenaturing Chromatography of GLUT1. Size-exclusion chromatography (SEC) was performed on a Toso Haas TSK-Gel G4000-SWXL column preequilibrated with 150 mM NaCl and 5 mM MOPS, pH 7.2, containing 20 mM cholate ± 10 mM DTT and developed at 0.3 mL·min^{-1}. The column was calibrated by using protein standards of known Stokes radii. Lectin chromatography of cholate-solubilized GLUT1 was performed on a wheat germ lectin–Sepharose 4B column (7 cm × 1 cm) equilibrated with 25 mM NaCl, 5 mM Tris-HCl, and 10 mM cholic acid, pH 7.4. The 45000*g* supernatant (1 h) of cholate-solubilized GLUT1 (295 μL, 34 μg) was applied to the column, and samples of eluate were collected at a rate of 20 mL·h^{-1}. GLUT1 was eluted from the column with 500 mM *N*-acetylglucosamine.

Sedimentation Velocity Studies of GLUT1. GLUT1 was solubilized in 20 mM cholic acid and centrifuged at 200000*g* for 1 h at 4 °C, and the supernatant was placed on top of a 5–20% sucrose gradient in 150 mM NaCl and 5 mM MOPS, pH 7.2, containing 20 mM cholic acid. The gradients were centrifuged for 18 h at 4 °C and 40000 rpm with a Beckman ultracentrifuge and SW 50.1 rotor. Gradients were fractionated with an ISCO fractionator. GLUT1 was detected by ELISA. $s_{20,w}$ was calculated by the method of Fritch (1973).

Analytical Procedures. Protein content was determined by a modified Lowry procedure (Carruthers & Helgerson, 1989). Phospholipid phosphorus content was determined by a modified Bartlett procedure (Carruthers & Melchior, 1984a). Lipid acyl-chain composition and content were determined by gas chromatography (Carruthers & Melchior, 1984a). [^{3}H]Cytochalasin B binding to reconstituted GLUT1 was determined as described by Helgerson and Carruthers (1987). SDS–PAGE of membrane proteins and GLUT1 was as described previously (Carruthers & Helgerson, 1989). Immuno-(Western) blotting of proteins using δ- or C-antisera was as described in Harrison et al. (1990).

Results

Catalytic Activity. The transport activity of reconstituted GLUT1 purified in the absence (GLUT1 – DTT) or presence (GLUT1 + DTT) of DTT was measured at 0.1 mM D-glucose ± 10 μM cytochalasin B (a potent transport inhibitor). Reconstituted transport in EPC proteoliposomes is characterized by a $K_{m(app)}$ of ≈10 mM at room temperature (Carruthers & Melchior, 1984a,b). Thus sugar uptake at 0.1 mM D-glucose is subsaturating and is well approximated by the relationship $v = \pi$[D-glucose], where π is the limiting permeability of the system described by $\pi = V_{max}/K_{m(app)}$.

The experimentally determined values for cytochalasin B inhibitable, reconstituted glucose (0.1 mM) uptake at 100 μg of GLUT1/30 mg of EPC or at 5 mg of erythrocyte ghost protein/30 mg of EPC are $\pi = 0.015 \pm 0.002$ s^{-1} (GLUT1 + DTT), $\pi = 0.016 \pm 0.003$ s^{-1} (GLUT1 – DTT), and $\pi = 0.017 \pm 0.002$ s^{-1} (ghost proteins). D-Glucose-inhibitable cytochalasin B binding to the three reconstituted preparations is quantitatively indistinguishable, being characterized by $K_{d(app)} = 364 \pm 53$ nM and $B_{max} = (17.5 \pm 0.8$ pmol of cy-

tochalasin B)(μg of reconstituted GLUT1)$^{-1}$.

The turnover number ($k_{cat} = V_{max}/[GLUT1]$) for red cell sugar transport at 20 °C is 158–792 s^{-1} (Carruthers, 1990). Assuming $K_{m(app)}$ for reconstituted transport in EPC vesicles is 10 mM, the corresponding values for reconstituted transport are 17.4 s^{-1} (GLUT1 + DTT), 18.6 s^{-1} (GLUT1 – DTT), and 19.7 s^{-1} (ghost proteins; assuming GLUT1 comprises 2% of the total membrane protein mass). The low turnover numbers for reconstituted, GLUT1-mediated sugar transport are those expected for GLUT1 residing in EPC bilayers (Carruthers & Melchior, 1987).

SDS–PAGE of Purified GLUT1. GLUT1 + DTT is resolved by Coomassie staining and by immunoblot analysis as a broad band of average molecular mass 55 kDa upon reducing, discontinuous SDS–PAGE. GLUT1 – DTT is resolved as 55- and 110-kDa species upon reducing SDS–PAGE. Electroelution of the 55-kDa GLUT1 – DTT species followed by an additional round of SDS–PAGE results in formation of 55- and 110-kDa species. Nonreducing SDS–PAGE of both GLUT1 + DTT and GLUT1 – DTT reduces the amount of GLUT1 that penetrates the resolving gel but is otherwise without effect on the electrophoretic profile of GLUT1 penetrating the resolving gel.

Nondenaturing Chromatography. SEC of GLUT1 + DTT in cholate (20 mM) resolves GLUT1 as a single major peak of average Stokes' radius 5.74 nm. Cholate SEC of GLUT1 – DTT resolves GLUT1 as two poorly separated peaks of average Stokes' radii 5.74 and 7.48 nm (Figure 1). When GLUT1 – DTT is solubilized and chromatographed in the presence of DTT (10 mM), the larger, 7.48-nm particle becomes less prominent while the smaller 5.74-nm particle becomes more prominent. Both GLUT1 + DTT and GLUT1 – DTT are ligand binding competent. Maltose (200 mM, not shown) and D-glucose (200 mM) but not L-glucose (200 mM) inhibit photoincorporation of [^{3}H]cytochalasin B into both GLUT1 + DTT and GLUT1 – DTT (Figure 1). The bulk of labeling of GLUT1 – DTT appears to be accounted for by the 7.48-nm particle. As photolabeled GLUT1 + DTT is resolved as a single major peak of 5.74 nm, it is unlikely that the larger labeled peak of GLUT1 – DTT (7.48 nm) results from UV-induced aggregation of GLUT1 or from solubilization in cholate. Cholate SEC of cholate-solubilized red cell membrane proteins resolves GLUT1 and cytochalasin B photolabeled GLUT1 as a mixture of 5.74- (minor component) and 7.48-nm (major component) particles (Figure 1). This profile is unaffected by the presence of DTT (10 mM) during solubilization.

The bulk of the phospholipid present in the cholate-solubilized GLUT1 preparations elutes with a Stokes radius of 5.41 nm. The amount of lipid tightly associated with GLUT1 was measured by applying cholate-solubilized GLUT1 to a lectin column and collecting both flow-through and *N*-acetylglucosamine-eluted fractions. The bulk (92% by mass, 160 μg) of the phospholipid copurified with GLUT1 elutes from the column in the flow-through fraction. The remaining phospholipid (8% by mass, 14 μg) and 96% of the applied protein (33 μg) are eluted from the column by *N*-acetylglucosamine. Thus only 8% of the total phospholipid that copurifies with GLUT1 is closely associated with GLUT1. Assuming an average molecular weight for a phospholipid of 900, the molar ratio of associated phospholipid:GLUT1 is 26:1.

Sucrose Gradient Ultracentrifugation. GLUT1 + DTT solubilized in 20 mM cholate and subjected to sucrose gradient ultracentrifugation in 20 mM cholate is resolved into two major particle sizes. The major component is a 4.83S particle while the minor component is a 7.6S particle (Figure 2). The reverse profile is observed upon ultracentrifugation of GLUT1 – DTT (Figure 2).

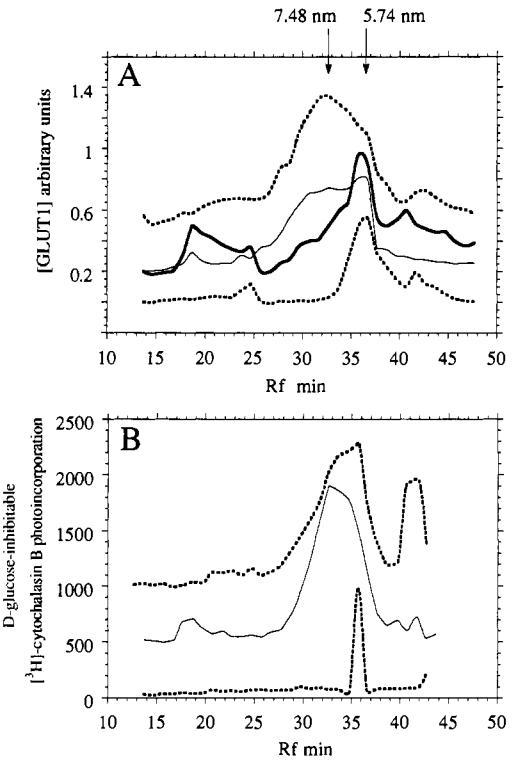

FIGURE 1: Size-exclusion chromatography of cytochalasin B photolabeled, cholate-solubilized GLUT1 from red cell membranes or from purified GLUT1 preparations. (A) Elution profile of GLUT1 detected by ELISA using C- and δ-antibodies. Ordinate: [GLUT1] in arbitrary units. Abscissa: retention time in minutes. Four data sets are shown and have been displaced in the *y*-axis in order to facilitate distinction. The lowest curve (---) shows the chromatographic profile of GLUT1 + DTT (≈20 μg). The middle curves (solid lines) show the chromatographic profiles of GLUT1 – DTT (≈20 μg) when solubilized and chromatographed in the absence (thin line) or presence (thick line) of dithiothreitol (10 mM). The uppermost curve (---) shows the chromatographic profile of GLUT1 solubilized from erythrocyte ghosts. The flow rate was 0.3 mL/min. The column was calibrated with Pharmacia high and low molecular weight gel filtration calibration kits. Stokes' radius (nm) is obtained as $21.672 - 0.4341R_f$ (correlation coefficient = 0.965). The arrows indicate the retention times of 7.48- and 5.74-nm particles. With this column, these retention times correspond to $K_{av} = 0.584$ and 0.445, respectively. (B) Elution profile of [^{3}H]cytochalasin B photolabeled GLUT1. Ordinate: cpm photoincorporated in the presence of 200 mM L-glucose minus cpm photoincorporated in the presence of 200 mM D-glucose. Abscissa: retention time in minutes. Three data sets are shown and have been displaced in the *y*-axis in order to facilitate distinction. The lowest curve (---) shows the chromatographic profile of label photoincorporated into GLUT1 + DTT (≈20 μg). The middle curve (solid line) shows the chromatographic profile of label photoincorporated into GLUT1 – DTT (≈20 μg) when solubilized and chromatographed in the absence of dithiothreitol. The uppermost curve (---) shows the chromatographic profile of label photoincorporated into GLUT1 solubilized from erythrocyte ghosts. These data were obtained by analyzing the fractions obtained by (A) for associated [^{3}H]cytochalasin B. Integration of the areas under each curve allows estimates of relative efficiency (% total cpm/% total protein) of photoincorporation of cytochalasin B per unit 5.74-nm or per unit 7.48-nm complex. These values are GLUT1 + DTT, 0.96 (5.74 nm); GLUT1 – DTT, 0.95 (5.74 nm), 0.97 (7.48 nm); and ghosts, 1.63 (5.74 nm), 0.61 (7.48 nm).

Discussion

The physical properties of the purified erythrocyte glucose transport protein (GLUT1) are critically dependent upon the presence of reductant during purification. When purified in

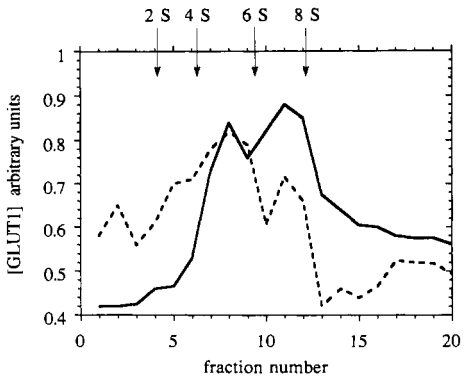

FIGURE 2: Sucrose gradient ultracentrifugation of 10 μg of GLUT1 + DTT and GLUT1 - DTT in linear (5–20%) sucrose gradients. Ordinate: [GLUT1] detected by ELISA in arbitrary units. Abscissa: fraction number. The solid curve shows the results obtained with GLUT1 - DTT and the dashed curve shows the results obtained with GLUT1 + DTT. The arrows indicate the calculated positions of particles of defined sedimentation coefficients ($s_{w,20}$) in Svedberg units. When the 4.83S particles of both GLUT1 + DTT and GLUT1 - DTT preparations are analyzed by SEC (as in Figure 1), they are resolved as 5.7-nm complexes. When the 7.6S particles of both GLUT1 + DTT and GLUT1 - DTT preparations are analyzed by SEC (as in Figure 1), they are resolved as 7.5-nm complexes. This experiment is typical of four separate experiments.

the presence of reductant, cholate-solubilized GLUT1 is resolved as a single major species of average Stokes' radius 5.74 nm and sedimentation coefficient 4.83×10^{-13} s. When purified in the absence of reductant, GLUT1 is resolved as two species. The major species is of average Stokes' radius 7.5 nm and sedimentation coefficient 7.6×10^{-13} s. This species is resolved as a broad peak and is almost certainly comprised of a distribution of particle sizes. The minor species is that found with transporter purified in the presence of DTT. The 5.74-nm species of GLUT1 - DTT can be enriched at the expense of the 7.48-nm species by solubilization of GLUT1 - DTT in the presence of DTT.

Each solubilized glucose transporter is associated with 26 molecules of lipid. With the methods described in this study, the quantity of cholic acid associated with the solubilized GLUT1–lipid complex is too low to measure accurately due to the high cmc of cholate. However, assuming GLUT1 is surrounded by an annulus of lipid bilayer and that 1 mol of phospholipid is solubilized by 2 mol of cholate (see Materials and Methods), a lower limit of cholate associated with the lipid–GLUT1 complex is 52 mol of cholate: 1 mol of GLUT1. A lower estimate of the molecular mass of the GLUT1–lipid–cholate complex is thus 99 kDa (assuming an average molecular mass of monomeric GLUT1 of 55 kDa).

On the basis of these measurements and assumptions, we conclude that the major complex of GLUT1 + DTT contains dimeric GLUT1 and that the major complex of GLUT1 - DTT contains tetrameric GLUT1 (Table I). If our estimate of bound detergent per complex is 5-fold too low, these sizes would fall to monomeric and dimeric GLUT1, respectively. If our estimate of the GLUT1 partial specific volume (v_P = 0.75 $cm^3 \cdot g^{-1}$) is 7% too high due to extensive glycosylation (Spiro, 1973), these sizes would fall to 1.7 and 3.6 units of GLUT1 per complex.

Cholate-solubilized human erythrocyte ghost glucose transport proteins are resolved as both 5.7- and 7.5-nm particles. The major species present is the 7.5-nm complex. Solubilized GLUT1 from ghost membranes thus closely resembles solubilized GLUT1 - DTT. This conclusion is based upon detection of GLUT1 by immunologic and by cytochalasin B photoincorporation experiments.

Table I: Hydrodynamic Properties of the Solubilized Glucose Transporter

parameters	GLUT1 + DTT[a]	GLUT1 - DTT[a]
Stokes radius (nm)	5.74	7.48
phospholipid binding (g/g of protein)	0.424	0.424
phospholipid binding (mol/mol of protein)	26	26
detergent binding[b] (mol/mol of protein)	52	52
diffusion coeff[c] ($D_{20,w}$) ($cm^2 \cdot s^{-1}$)	3.85×10^{-7}	2.96×10^{-7}
partial sp vol[d] ($cm^3 \cdot g^{-1}$)	0.807	0.807
sedimentation coeff (s_{20w}) (s)	4.83×10^{-13}	7.59×10^{-13}
mol wt[e]	189 594	411 217
protein moiety[f]	104 111	225 811
unit size[g] (monomers)	1.91	4.15
frictional ratio	1.369	1.383
max possible hydration[h] (g of $H_2O \cdot g^{-1}$)	1.27	1.33
max possible prolate a/b[i]	4.7	4.8

[a] Refers to the major component of solubilized GLUT1. [b] Calculated by assuming GLUT1 is surrounded by an annulus of lipid bilayer and 2 mol of cholate solubilizes 1 mol of lipid (see Materials and Methods). [c] The diffusion coefficient of the protein–lipid–cholate complex is calculated from the Stokes radius, combining the Einsteinn–Sutherland equation and Stokes' law. [d] The partial specific volume of GLUT1 (v_P) was calculated from the amino acid composition of the protein (Mueckler et al., 1985). The partial specific volumes of lipid (v_L, 0.975 $cm^3 \cdot g^{-1}$) and of cholate (v_D, 0.78 $cm^3 \cdot g^{-1}$) were taken from Hackenberg and Klingenberg (1980) and from Carey and Small (1972). The partial specific volume of the GLUT1–lipid–detergent complex (v^*) was calculated as $v^* = x_P v_P + x_L v_L + x_D x_D$, where x_P, x_L, and x_D are the weight fractions of the individual components (protein, lipid, and detergent). [e] The molecular weight (M) of the complex was calculated by using the Svedberg equation. [f] The molecular weight of the protein component of the complex was calculated as $x_P M$. [g] The unit size (oligomeric state) of the protein was calculated as $x_P M/55\,000$, assuming an average molecular weight of monomeric GLUT1 of 55 000. [h] Assuming the particle is a sphere, all excess friction is due to hydration. An upper limit of hydration (δ^{max}) is calculated as $\delta^{max} = v^*/v_w \cdot [(f/f_{min})^3 - 1]$, where v_w is the partial specific volume of water. [i] If the particle has no hydration, the axial ratio of the particle is the maximum possible. The axial ratio of prolate ellipsoids is found in tables of the Perrin factors with $F_{max} = f/f_{min}$.

A remaining paradox is the observation that the apparent size of GLUT1–lipid–detergent micelles released upon cholate solubilization of whole red cell membranes is unaffected by the presence of dithiothreitol. This could result from solubilization of GLUT1–peripheral protein heterocomplexes. Alternatively, the loss of peripheral membrane proteins or use of the detergent octyl glucoside during purification could render GLUT1 more susceptible to disulfide formation/breakdown upon solubilization. Future studies must address these possibilities.

Both large and small GLUT1 particles released upon cholate solubilization of ghosts and purified GLUT1 are ligand binding competent prior to solubilization and translocation competent following reintroduction into lipid bilayers. Our data demonstrate that GLUT1 - DTT and ghost membrane proteins (comprised largely of the 7.5-nm complex upon solubilization) possess quantitatively indistinguishable catalytic activity from GLUT1 + DTT (comprised largely of the 5.7-nm complex).

Fluorescence quenching studies show that GLUT1 - DTT and red cell membranes depleted of peripheral membrane proteins display two components of D-glucose binding (high and low affinity; Carruthers, 1986a,b) while GLUT1 + DTT displays a single component of sugar binding (intermediate affinity; Gorga & Lienhard, 1982; Hebert and Carruthers, unpublished). Cytochalasin B binding studies with intact red cells and with red cell ghosts (Helgerson & Carruthers, 1987) and sugar transport measurements with intact cells (Carruthers & Helgerson, 1991) demonstrate that maltose and cytochalasin B (nontransported, competitive inhibitors of sugar uptake and

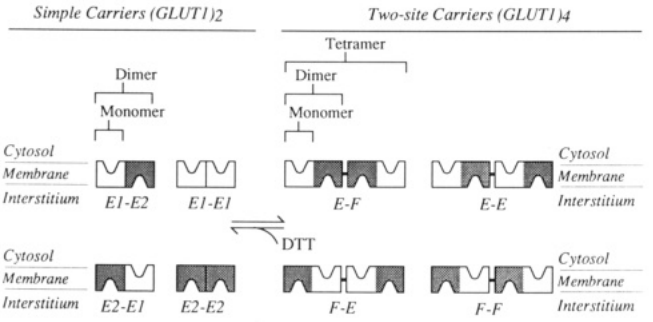

FIGURE 3: A model for the relationship between glucose carrier (GLUT1) oligomeric state and glucose carrier function. The glucose carrier can exist in two states: $(GLUT1)_2$, a dimer, and $(GLUT1)_4$, a tetramer. $(GLUT1)_2$ behaves as a simple carrier while $(GLUT1)_4$ behaves as a two-site carrier. $(GLUT1)_4$ is converted to $2(GLUT1)_2$ by dithiothreitol (DTT). Each monomer of $(GLUT1)_2$ and $(GLUT1)_4$ is presumed to be catalytically active. The sugar influx and sugar efflux sites of these glucose carriers are shown in schematic form. $(GLUT1)_2$ is a dimer of two simple carriers (GLUT1) where isomerizations of each monomer of the dimer between the sugar influx (E2) and sugar efflux (E1) conformations are independent. Thus four unliganded states of $(GLUT1)_2$ are possible. These are indicated in the figure. $(GLUT1)_4$ is a dimer of $(GLUT1)_2$. Dimerization of $(GLUT1)_2$, however, induces a significant change in dimer function. The binding sites of each monomer of the dimer are no longer independent and may show cooperativity in ligand binding. They become rearranged in an antiparallel fashion such that each dimer always presents an influx and an efflux site to available substrate. Isomerization of a monomer's influx site to an efflux site now promotes the coupled, antiparallel isomerization of the efflux site of the other monomer to an influx site and vice versa. Each dimer can thus exist in one of two states—E or F. The tetramer can thus exist in four possible unliganded states. These are indicated in the Figure. Each tetramer would always present two sugar influx and two sugar efflux sites to substrate.

sugar exit, respectively) display negative cooperativity in binding to the glucose transport system. Binding constants for maltose and cytochalasin B interaction with intact cell GLUT1 are very close to those for interaction with GLUT1 – DTT.

These data suggest the following: (1) Membranes from which the larger GLUT1 complex is solubilized contain glucose transporters characterized by multiple, interacting sugar transport sites. (2) Membranes from which the smaller GLUT1 complex is solubilized contain glucose transporters characterized by a single binding site (or multiple, noninteracting sites with identical affinity for D-glucose). (3) The intact cell sugar transport system resembles GLUT1 – DTT in its ligand-binding properties. (4) The presence of reductant during purification promotes conversion of the larger GLUT1 complex to the smaller complex. This could result from reduction of intra- or intermolecular disulfides.

Thus erythrocyte sugar transport may be mediated by a multimeric assembly of GLUT1 monomers (Figure 3). In the dimeric state, each GLUT1 monomer possesses catalytic activity, but the ligand binding sites do not interact cooperatively. In the tetrameric state each GLUT1 monomer possesses catalytic activity but interacts with other monomers to display cooperativity in ligand binding. Cooperative interactions are frequently observed in multimeric enzymes and ligand binding proteins where binding of a ligand to one subunit of the complex affects the affinity of the remaining subunit(s) for substrate (Imai, 1983; Lahue & Schachman, 1986).

Such a multimeric transport mechanism is quantitatively compatible with eukaryotic sugar transport systems (Carruthers, 1991). This model is based on the demonstrations (Helgerson & Carruthers, 1987; Carruthers & Helgerson, 1991) that transport is mediated by a carrier that simultaneously exposes sugar influx and sugar efflux sites to substrate. It is proposed that transport proceeds as coupled movements of substrate through discrete but interacting carrier subunits. Thus the transport system could be a dimer of two identical carrier units (see Figure 3) where substrate binding sites are arranged in an antiparallel fashion but where isomerization of one subunit promotes the antiparallel isomerization of the second. In the presence of reductant, these carrier units retain catalytic activity but are uncoupled and thus no longer display cooperativity in ligand binding.

REFERENCES

Birnbaum, M. J., Haspel, H. C., & Rosen, O. M. (1986) *Proc. Natl. Acad. Sci. U.S.A. 83*, 5784–5788.
Cairns, M. T., Elliot, D. A., Scudder, P. R., & Baldwin, S. A. (1984) *Biochem. J. 221*, 179–188.
Carey, M. C., & Small, D. M. (1972) *Arch. Intern. Med. 130*, 506–527.
Carruthers, A. (1986a) *Biochemistry, 25*, 3592–3602.
Carruthers, A. (1986b) *J. Biol. Chem. 261*, 11028–11037.
Carruthers, A. (1990) *Physiol. Rev. 70*, 1135–1176.
Carruthers, A. (1991) *Biochemistry 30*, 3898–3906.
Carruthers, A., & Melchior, D. L. (1984a) *Biochemistry 23*, 6901–6911.
Carruthers, A., & Melchior, D. L. (1984b) *Biochemistry 23*, 2712–2718.
Carruthers, A., & Melchior, D. L. (1987) *Annu. Rev. Physiol. 50*, 527–571.
Carruthers, A., & Helgerson, A. L. (1989) *Biochemistry 28*, 8337–8346.
Carruthers, A., & Helgerson, A. L. (1991) *Biochemistry 30*, 3907–3915.
Celenza, J. L., Marshall-Carlson, L., & Carlson, M. (1988) *Proc. Natl. Acad. Sci. U.S.A. 85*, 2130–2134.
Cuppoletti, J., Jung, C. Y., & Green, F. A. (1981) *J. Biol. Chem. 256*, 1305–1306.
Fritch, A. (1973) *Anal. Biochem. 55*, 57–64.
Gorga, F. R., & Lienhard, G. E. (1982) *Biochemistry 21*, 1905–1908.
Hackenberg, H., & Klingenberg, M. (1980) *Biochemistry 19*, 458–555.
Harrison, S. A., Buxton, J. M., Helgerson, A. L., MacDonald, R. G., Chlapowski, F. J., Carruthers, A., & Czech, M. P. (1990) *J. Biol. Chem. 265*, 5793–5801.
Helgerson, A. L., & Carruthers, A. (1989) *Biochemistry 28*, 4580–4594.
Helgerson, A. L., Hebert, D. N., Naderi, S., & Carruthers, A. (1989) *Biochemistry 28*, 6410–6417.
Imai, K. (1983) *J. Mol. Biol. 167*, 741–749.
James, D. E., Strube, M., & Mueckler, M. (1989) *Nature 338*, 83–87.
Jarvis, S. M., Ellory, J. C., & Young, J. D. (1986) *Biochim. Biophys. Acta 855*, 312–315.
Jung, C. Y., Hsu, T. L., Hah, J. S., Cha, C., & Haas, M. N. (1980) *J. Biol. Chem. 255*, 361–364.
Kayano, T., Fukumoto, H., Eddy, R. L., Fan, Y. S., Byers, M. G., Shows, T. B., & Bell, G. I. (1988) *J. Biol. Chem. 263*, 15245–15248.
Lahue, R. S., & Schachman, H. K. (1986) *J. Biol. Chem. 261*, 3079–3084.
Mueckler, M., Caruso, C., Baldwin, S. A., Panico, M., Blench, I., Morris, H. R., Allard, W. J., Lienhard, G. E., & H. F. L. (1985) *Science 229*, 941–945.
Spiro, R. G. (1973) *Adv. Protein Chem. 27*, 349–467.
Thorens, B., Sarkar, H. K., Kaback, H. R., & Lodish, H. F. (1988) *Cell 55*, 281–290.